

# Accepted Manuscript

Discovery of novel NO-releasing celastrol derivatives with Hsp90 inhibition and cytotoxic activities

Na Li, Manyi Xu, Na Bao, Wei Shi, Qixing Li, Xiaowei Zhang, Jianbo Sun, Li Chen



PII: S0223-5234(18)30875-4

DOI: [10.1016/j.ejmech.2018.10.013](https://doi.org/10.1016/j.ejmech.2018.10.013)

Reference: EJMECH 10799

To appear in: *European Journal of Medicinal Chemistry*

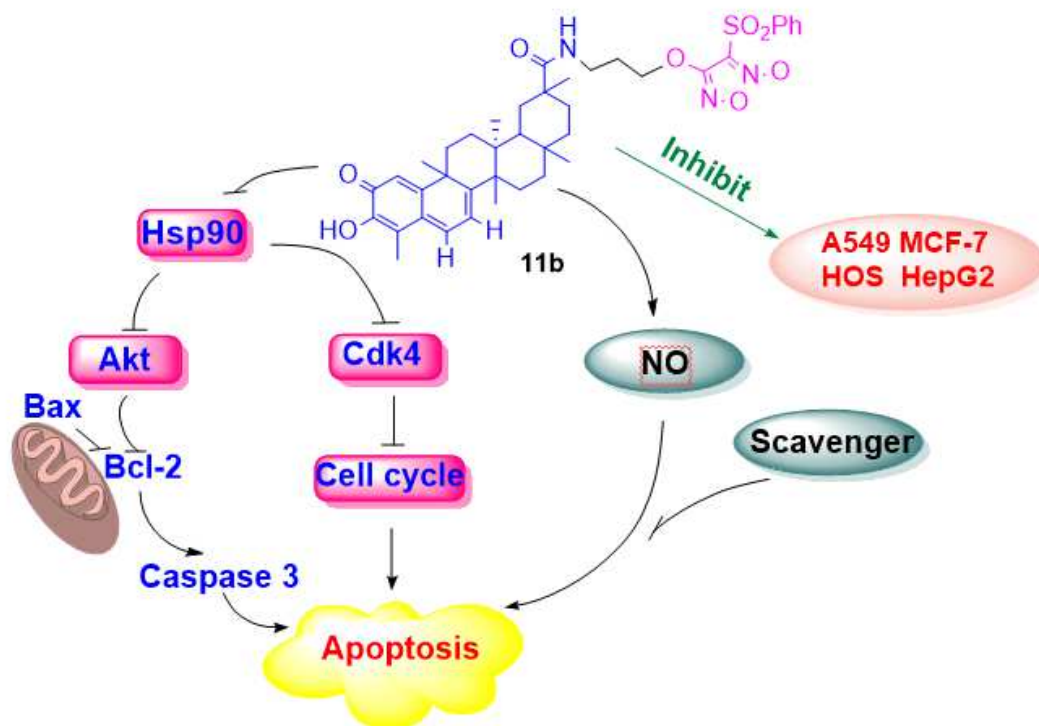
Received Date: 14 August 2018

Revised Date: 1 October 2018

Accepted Date: 5 October 2018

Please cite this article as: N. Li, M. Xu, N. Bao, W. Shi, Q. Li, X. Zhang, J. Sun, L. Chen, Discovery of novel NO-releasing celastrol derivatives with Hsp90 inhibition and cytotoxic activities, *European Journal of Medicinal Chemistry* (2018), doi: <https://doi.org/10.1016/j.ejmech.2018.10.013>.

This is a PDF file of an unedited manuscript that has been accepted for publication. As a service to our customers we are providing this early version of the manuscript. The manuscript will undergo copyediting, typesetting, and review of the resulting proof before it is published in its final form. Please note that during the production process errors may be discovered which could affect the content, and all legal disclaimers that apply to the journal pertain.



A series of celastrol/NO donor hybrids were designed, synthesized and evaluated. **11b**, which released the highest level of NO *in vitro*, exhibited the best antiproliferative effects. The results suggested that inhibition of Hsp90 and release of NO was synergistic in cancer cells.

# Discovery of Novel NO-releasing Celastrol Derivatives with Hsp90 Inhibition and Cytotoxic Activities

Na Li, Manyi Xu, Na Bao, Wei Shi, Qixing Li, Xiaowei Zhang, Jianbo Sun\*, and Li Chen\*

State Key Laboratory of Natural Medicines, Department of Natural Medicinal Chemistry, China Pharmaceutical University, 24 Tong Jia Xiang, Nanjing 210009, People's Republic of China

\* Corresponding author: Tel: +86 83271447

E-mail address: [sjbcpu@gmail.com](mailto:sjbcpu@gmail.com) (Jianbo Sun); [chenli627@cpu.edu.cn](mailto:chenli627@cpu.edu.cn) (Li Chen)

Keywords: Celastrol, Nitric oxide, Hsp 90, Apoptosis, Cytotoxicity

## ABSTRACT

To develop multifunctional drugs, a series of celastrol/NO donor hybrids were designed, synthesized and evaluated. The detection of NO release amounts showed that more NO of these hybrids released, the more tumor cells were inhibited. **11b**, which released the highest level of NO *in vitro*, exhibited superior potency ( $IC_{50} = 0.48 \pm 0.06 \mu\text{M}$ ) compared to the other compounds. Further pharmacological studies showed that **11b** induced dysregulations of the Hsp90 clients (Akt and Cdk4), apoptosis, and cell cycle arrested at G<sub>0</sub>/G<sub>1</sub> phase against A549 cells. These results suggested that inhibition of Hsp90 and release of NO was synergistic in cancer cells. Overall, the NO-releasing capacity and the inhibition of Hsp90 pathway signaling might explain the potent anti-proliferative activities of these compounds.

## 1. Introduction

Celastrol (CEL) is a triterpenoid isolated from the root extracts of Thunder of God Vine (*Tripterygium wilfordii* Hook F.). It has been widely investigated about its anti-proliferative activity [1-3]. A recent report demonstrated that the

anti-proliferative activity of CEL results from targeting the Hsp90 (Heat shock protein 90) signaling pathways [4-5]. Hsp90 is a protein chaperone that helps its clients to maintain their correct conformation [6-7]. Many of Hsp90 clients are demonstrated as oncogenic proteins, such as protein kinase B (Akt), cyclin-dependent kinases 4 (Cdk4), epidermal growth factor receptor (EGFR), Her-2, c-Met [8]. Thus, CEL can regulate multiple signaling pathways simultaneously to inhibit the proliferation of cancer cells.

Nitric oxide (NO) is a key signaling and effector molecule in the development of tumors [9]. Generally, high levels of NO can induce apoptosis in tumor cells while lower concentrations of NO usually protect cells [10, 11]. It has been reported that NO regulates several cancer-related signaling pathways, such as, Akt, extracellular signal-regulated kinases (ERKs), mammalian target of rapamycin (mTOR), cyclin D1/retinoblastoma (Rb) [12-13]. In addition, NO-donating hybrids can significantly decrease the resistant rates of their parent drugs [14]. Thus, many chemical NO donors have been designed to generate high levels of NO intracellular [15]. Among them, furoxan, which is widely used in the creation of drugs, can inhibit the proliferation of cancer cells through generation of large amounts of NO [15]. In recent decades, many hybrids from furoxan based NO donor displayed potent antitumor activity [16-18]. For example, the  $IC_{50}$  value of  $\beta$ -elemene/furoxan hybrid (0.002  $\mu$ M) was much superior to that of  $\beta$ -elemene (197.65  $\mu$ M). Moreover, this hybrid significantly suppressed the tumor growth *in vivo* [19]. Hence, generation of furoxan based hybrids is an effective strategy for the treatment of cancer.

Hybridization strategy, a well-known approach in drug design, allows a combination of two or more pharmacophores with bioactive scaffolds to generate a single molecular architecture. Generally, these hybrids possess improved affinity and activity in comparison to their parent compounds. This strategy has been widely used in the development of antibacterial, anticancer and antimalarial drugs [20-21]. In order to develop novel anti-tumor drugs, hybrids based on natural products have been extensively studied [22-24]. Recently, many studies reported that the hybrids of triterpenoid and a NO donor showed enhanced anti-proliferative activities compared to the parent compound [25-28]. However, the combination of CEL and NO donor

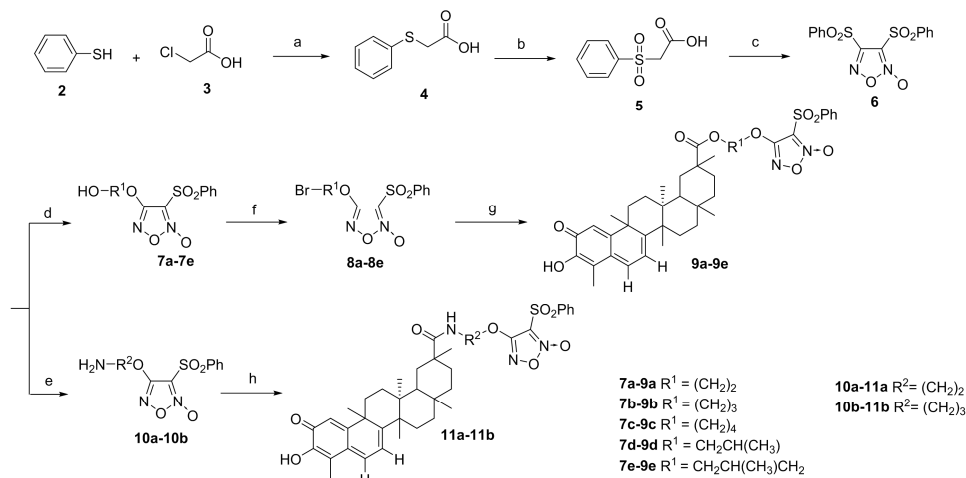
have not been reported. Thus, on the basis of the analysis above and the hybridization strategy, the furoxan based NO donor was introduced at 29-position of CEL by esterification and amidification of 20-carboxylic acid (**9a-11b**) to synthesize celastrol/furoxan hybrids (Scheme 1). Furthermore, nitrate, another type of NO donor, was also linked to CEL (**13a-13d**, Scheme 2). Their anti-proliferative activities were assayed *in vitro*. Moreover, cell cycle arrest, apoptosis, NO-releasing ability and the inhibition of Hsp90 clients of **11b** were biologically evaluated to reveal the mechanisms of action of these hybrids.

## 2. Results and discussion

### 2.1. Chemistry

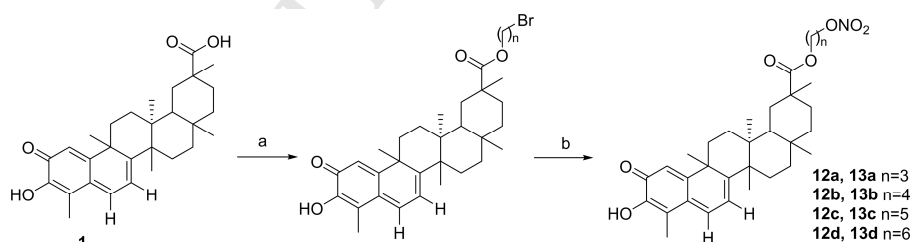
The synthesis of hybrids **9a-e** and **11a-11b** was provided in Scheme 1. The condensation of benzenethiol (**2**) and chloroacetic acid (**3**) under basic conditions generated 2-(phenylthio) acetic acid (**4**) which was subjected to further oxidation in 30% hydrogen peroxide (H<sub>2</sub>O<sub>2</sub>) aqueous solution to provide 2-(phenylsulfonyl) acetic acid (**5**) [29]. **5** was converted to diphenylsulfonyl-furoxan (**6**) by treatment with fuming nitric acid (HNO<sub>3</sub>) [29]. **6** then reacted with corresponding diols or amines to produce the indicated compounds (**7a-7e**, **10a-10b**) [29]. **7a-7e** was treated with triphenylphosphine (PPh<sub>3</sub>) and carbon tetrabromide (CBr<sub>4</sub>) to give **8a-8e** [30]. CEL (**1**) further reacted with **8a-8e** under basic conditions to provide **9a-9e** [31]. Compounds **11a** and **11b** were obtained by coupling **1** with **10a-10b** catalyzed by benzotriazol-1-yl-oxytripyrrolidinophosphonium hexafluorophosphate (PyBop) with the presence of Hunig's base [31]. Then, piperazine and piperidine were used as the linkers. However, the intermediates couldn't react with CEL with the presence of PyBop and Hunig's base or 1-ethyl-3-(3-dimethylaminopropyl)carbodiimide hydrochloride (EDCI) and 1-Hydroxybenzotriazole (HOBT) (S-scheme 1). In order to increase the reactivity of CEL, we try to convert the carboxylic acid of CEL to acyl chloride with thionyl chloride (SOCl<sub>2</sub>) or oxalyl chloride [(COCl)<sub>2</sub>] (S-scheme 1). The results showed that the structure of CEL was broken by the above reagents. Next, 2-methylaminoethanol was used to introduce furoxan (S-scheme 1). Unfortunately, this reaction was failed again. These results indicated that the increasing steric

hindrance of the intermediates might prevent the processes of the reactions. Thus, we gave up introducing the other amines to CEL.



**Scheme 1.** Reagents and conditions (a) NaOH, reflux, 1 h; (b) H<sub>2</sub>O<sub>2</sub>, rt, 3 h; (c) fuming HNO<sub>3</sub>, 100 °C, 4 h; (d) corresponding diols, 25% NaOH, -15 °C, 3 h; (e) corresponding amines, DBU, DCM, -15 °C, 3 h; (f) PPh<sub>3</sub>, CBr<sub>4</sub>, DCM, rt, 1 h; (g) **1**, NaHCO<sub>3</sub>, DMF, rt, 12 h; (h) **1**, PyBop, Hunig's base, DCM, rt, 10 h.

**1** was conducted esterification with the indicated dibromides on the carboxyl to provide **12a-12d** [32]. Compounds (**12a-12d**) were further transformed to the corresponding hybrids **13a-13d** [33], respectively, with silver nitrate (AgNO<sub>3</sub>) in acetonitrile (CH<sub>3</sub>CN) (Scheme 2).



**Scheme 2.** Reagents and conditions: (a) Br(CH<sub>2</sub>)<sub>n</sub>Br, NaHCO<sub>3</sub>, rt, 12 h; (b) AgNO<sub>3</sub>, 80 °C, CH<sub>3</sub>CN, 10 h.

## 2.2. *In vitro* anti-proliferative activity

We first detected the anti-proliferative effects of **1** and the derivatives against four tumor cell lines (A549, HOS, MCF-7 and HepG2) by MTT method. CDDO-Me, which was studied in phase III clinical trial, was used as positive control. As shown in Table 1, generally celastrol/nitrate hybrids (**13a-13d**) displayed moderate anti-proliferative activities compared to celastrol/furoxan hybrids (**9a-9e** and

**11a-11b**). Furthermore, two celastrol/furoxan hybrids (**11a** and **11b**), whose carboxylic acid (C-20) was connected with amino, displayed more potent anti-proliferative activities than the other hybrids. These results suggested that the amide linkage might be more appropriated for the modification of CEL in this study. Furthermore, introductions of different types of NO donors to the structure of CEL brought different influences to the activity. Among all target compounds, **11b** displayed more potent activity ( $IC_{50} = 0.48 \pm 0.06$ ,  $0.78 \pm 0.08$ ,  $0.51 \pm 0.09$  and  $1.41 \pm 0.18 \mu\text{M}$ ) in A549, MCF-7, HOS, and HepG2 cell lines. Thus, **11b** was selected for further investigation.

**Table 1**

Anti-proliferative activity of all the compounds against four cancer cell lines.

| Comp.                | Cytotoxicity $IC_{50}$ ( $\mu\text{M}$ ) <sup>a</sup> |                 |                 |                 |
|----------------------|---|-----------------|-----------------|-----------------|
|                      | A549  | MCF-7           | HOS             | HepG2           |
| <b>9a</b>            | $2.28 \pm 0.21$                                       | $2.76 \pm 0.32$ | $1.69 \pm 0.24$ | $4.75 \pm 0.81$ |
| <b>9b</b>            | $2.89 \pm 0.33$                                       | $2.12 \pm 0.24$ | $1.87 \pm 0.21$ | $4.53 \pm 0.22$ |
| <b>9c</b>            | $2.46 \pm 0.37$                                       | $3.95 \pm 0.31$ | $2.47 \pm 0.11$ | $3.53 \pm 0.39$ |
| <b>9d</b>            | $2.07 \pm 0.23$                                       | $2.02 \pm 0.36$ | $3.03 \pm 0.32$ | $2.39 \pm 0.31$ |
| <b>9e</b>            | $1.11 \pm 0.23$                                       | $1.49 \pm 0.15$ | $1.67 \pm 0.13$ | $2.39 \pm 0.33$ |
| <b>11a</b>           | $1.08 \pm 0.15$                                       | $1.52 \pm 0.22$ | $1.47 \pm 0.16$ | $3.82 \pm 0.42$ |
| <b>11b</b>           | $0.48 \pm 0.06$                                       | $0.78 \pm 0.08$ | $0.51 \pm 0.09$ | $1.41 \pm 0.18$ |
| <b>13a</b>           | $3.22 \pm 0.23$                                       | $2.54 \pm 0.33$ | $1.37 \pm 0.13$ | $1.85 \pm 0.17$ |
| <b>13b</b>           | $4.21 \pm 0.34$                                       | $3.82 \pm 0.37$ | $2.43 \pm 0.22$ | $6.08 \pm 0.35$ |
| <b>13c</b>           | $5.32 \pm 0.11$                                       | $3.01 \pm 0.43$ | $2.90 \pm 0.16$ | $3.40 \pm 0.56$ |
| <b>13d</b>           | $3.67 \pm 0.32$                                       | $3.17 \pm 0.32$ | $3.36 \pm 0.21$ | $4.71 \pm 0.27$ |
| <b>1</b>             | $1.57 \pm 0.15$                                       | $1.56 \pm 0.16$ | $0.93 \pm 0.03$ | $1.62 \pm 0.19$ |
| CDDO-Me <sup>b</sup> | $0.45 \pm 0.01$                                       | $0.79 \pm 0.21$ | $0.57 \pm 0.12$ | $0.33 \pm 0.02$ |

<sup>a</sup> MTT methods, cells were incubated with corresponding compounds for 48 h.  $IC_{50}$  ( $\mu\text{M}$ ) values (means  $\pm$  SD, n = 3).

<sup>b</sup> Positive control.

### 2.3. NO generation measurement

To explore the association between NO release amounts of these hybrids and their anti-proliferative activities, the NO release levels of these hybrids *in vitro* were detected using a Nitrate/Nitrite assay according to the standard curve. As shown in Fig. 1A, NO release amounts of the partial hybrids (4  $\mu\text{M}$  of **9a**, **9e**, **11a-b** and **13a-b**)

were increased continuously for 24 hours. However, the NO amounts declined slightly with further incubation. Thus, we decided to evaluate the cellular levels of NO of all celastrol/NO donor hybrids at 4  $\mu\text{M}$  for 24 h (Fig. 1B). It was observed that the hybrids designed in this study could produce different levels of NO intracellularly which generally agreed with the anti-proliferative activities.

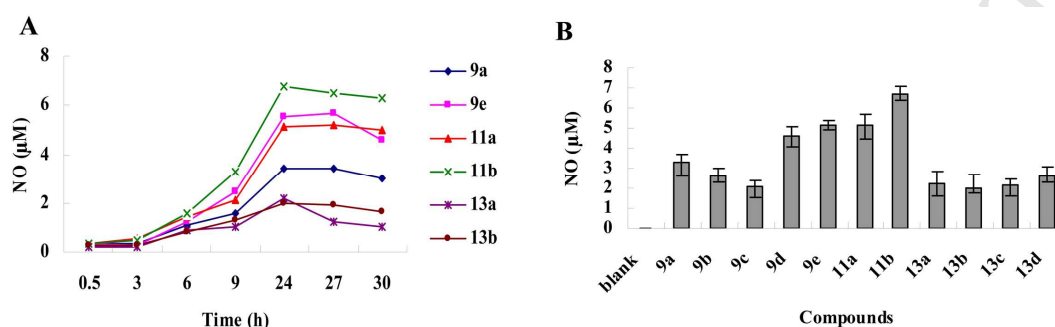


**Fig. 1.** Effects of NO produced by the target compounds on A549 cell proliferation. (A) NO release amounts of partial hybrids producing vs. time. A549 cells were treated with 4  $\mu\text{M}$  of the selected compounds for different hours (mean  $\pm$  SD,  $n = 3$ ). (B) The levels of NO produced by all of the compounds in A549 cells. A549 cells were treated with 4  $\mu\text{M}$  of all the hybrids for 24 hours (mean  $\pm$  SD,  $n = 3$ ).

In order to further demonstrate that the improved cytotoxicity of tumor cells was due to the high NO release amounts, an NO scavenger (PTIO) was introduced in the MTT assay [34]. Different concentrations of PTIO was added to the A549 cells for 2 h and then incubated with **11b** (4  $\mu\text{M}$ ) for another 24 h. Next the anti-proliferative activities were evaluated (Fig. 2). The results showed that the NO scavenger could decrease the anti-proliferation of **11b** dose-dependently in A549 cells. Thus, NO release amounts were contributed to the enhanced activity of **11b** in A549, which was consistent with the design strategy in this study.

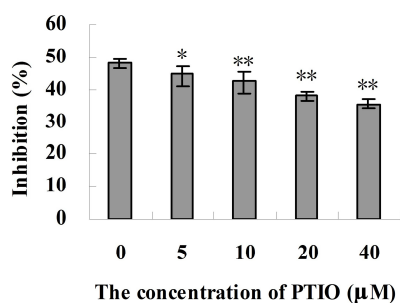


**Fig. 2.** Effect of PTIO on the anti-proliferative activity of **11b**. A549 cells were pretreated with the indicated concentrations of PTIO for 2 h and then treated with 4  $\mu\text{M}$  of **11b** for another 24 h. Data were expressed as the mean  $\pm$  SD (n=3). \* $P < 0.05$ , \*\* $P < 0.01$  vs. the group without PTIO.

#### 2.4. Effect of **11b** on Hsp90 client proteins

In the NO release assay, **11b** still remained anti-proliferative against A549 cells in the presence of high concentration of PTIO. We speculated that this activity might be derived from the parent compound (CEL). CEL could inhibit the pathway of Hsp90 to induce physiological apoptosis of the cells. We next evaluated whether the **11b** also inherited such ability. Cdk4 and *p*-Akt, as important clients of Hsp90, were measured by western blotting. As shown in Fig. 3A & B, **11b** significantly reduced the levels of Cdk4 and *p*-Akt in A549 cells. However, **11b** didn't inhibit Hsp90 directly. These results indicated that **11b** might target the Hsp90 chaperoning machinery, which was similar to CEL [35-37]. In this assay, we also observed that the Akt inhibitory activity of **11b** was stronger than that of CEL. The mechanism might be complex and was worthy of further investigation.

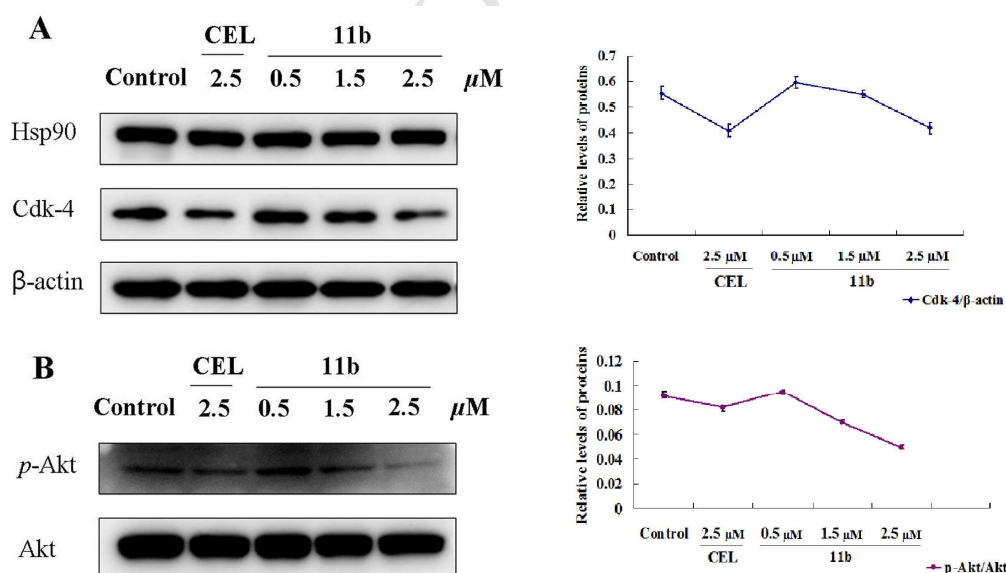


**Fig. 3.** Effects of **11b** on Hsp90 clients in A549 cells. A549 cells were treated with varying concentrations of **11b** for 24 h. (A) The expressions of Cdk-4 and Hsp90 were determined by Western Blotting using specific antibodies.  $\beta$ -actin was used as internal control; (B) The expressions of *p*-Akt and Akt were determined by Western Blotting

using specific antibodies.

## 2.5. Synergism of inhibition of Hsp90 and release of NO in **11b**

To evaluate whether inhibition of Hsp90 and release of NO of **11b** was synergistic in cancer cells, the two moieties of **11b** (**1** and **10b**) and their mixture (1:1) were examined for their anti-proliferative activities against A549 cells (MTT assay). As shown in Fig. 4, the inhibitory activities of **1**, **10b** and their mixture were much less potent compared to **11b**, respectively. These results showed that inhibition of Hsp90 and release of NO of **11b** was synergistic in this study.

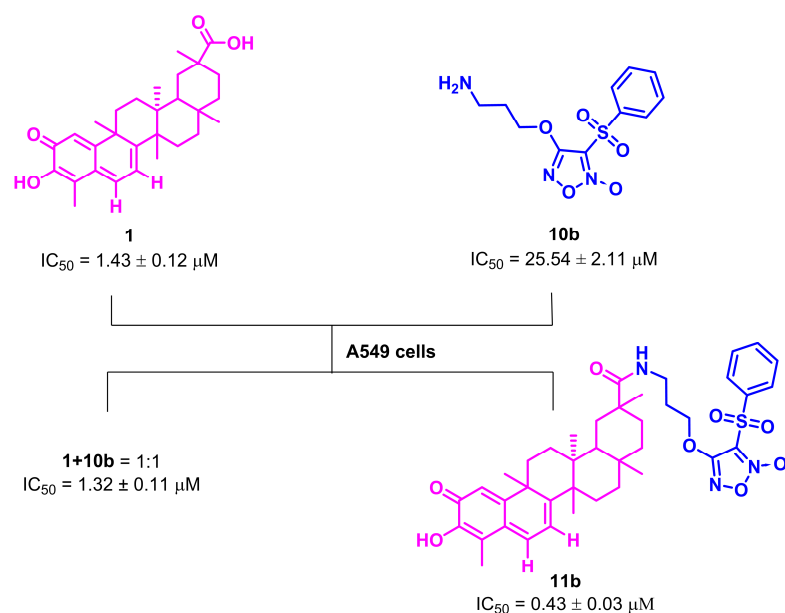


**Fig. 4.** Anti-proliferative activity of **11b** in comparison with that of **1**, **10b** and their mixture in A549 cells.

## 2.6. The morphological apoptosis induced by **11b**

As mentioned above, **11b** not only inhibited Hsp90 clients (*p*-Akt and Cdk4) but also released NO *in vitro*. Both of these two capabilities could induce the apoptosis of cancer cells. Therefore, the morphological apoptosis induced by **11b** was investigated by Hoechst 3342 staining. As shown in Fig. 5, Hoechst 3342 stained the apoptotic cells (bright blue) which appeared nuclear fragmentation and chromatin condensation in A549 cells. All of the images were magnified for the observation of cell morphology and the original photos were shown in Fig. S34-37.

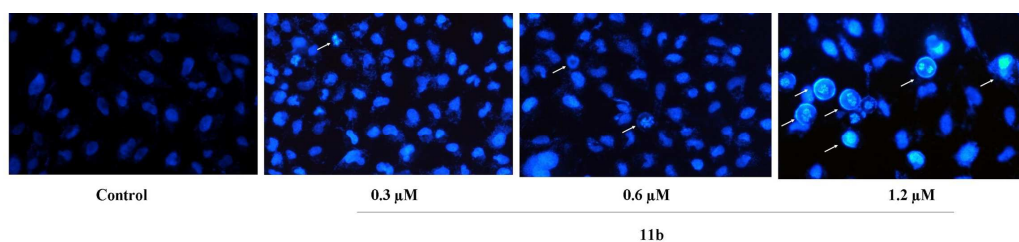


**Fig. 5.** Fluorescence microscopy images of A549 cells stained by Hoechst 33342. A549 cells were treated with the **11b** at indicated concentrations for 48 h.

### 2.7. Effect of **11b** on cell apoptosis

Then, the apoptosis induced by **11b** was tested and compared with that of CEL. Flow cytometry assay was performed to analyze the apoptotic cells mediated by **11b** and CEL in A549 cells. As shown in Fig. 6A, **11b** induced apoptosis in a dose-dependent manner in A549 cells. At the concentration of 1.2  $\mu\text{M}$  (Fig. 6B), the early and late apoptosis cells account for 12.9 % and 31.0 % respectively, which were much higher than that of CEL (7.8 %; 11.2 %). Thus, introduction of NO donor to CEL could promote the apoptosis of cancer cells.

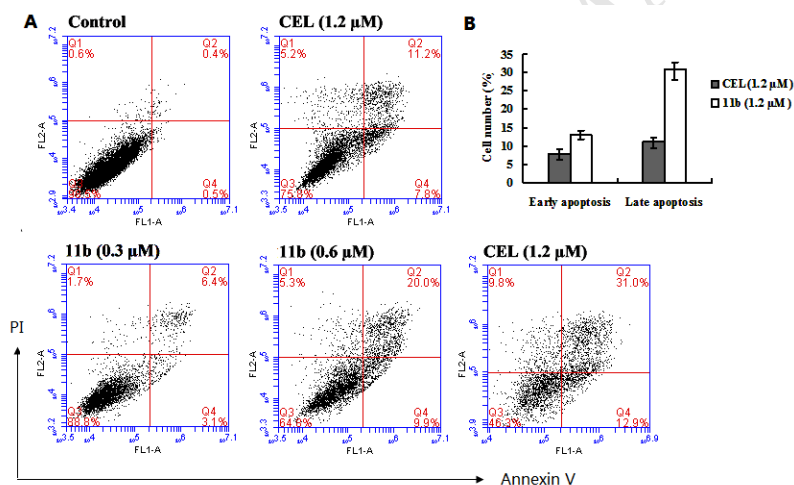


**Fig. 6.** Effect of **11b** on apoptosis of A549 cells. (A) A549 cells were treated with **11b** at the indicated concentrations for 48 h. Apoptotic effects were measured by flow cytometry using Annexin V-FITC/PI staining protocol; (B) Representative histograms for the numbers of cells (% of total) in the early and late stages of apoptosis for the treatment groups.

### 2.8. Effect of **11b** on cell cycle

From the results illustrated in Fig. 3, **11b** could inhibit the expression of Cdk4 which is a regulator protein of cell cycle. In order to further investigate the

mechanism of its anti-proliferative activity, the effect of **11b** on the cell cycle progression was evaluated. As shown in Fig. 7, **11b** arrested cell cycle at G<sub>0</sub>/G<sub>1</sub> phase in A549 cells, which was another pathway to induce apoptosis.

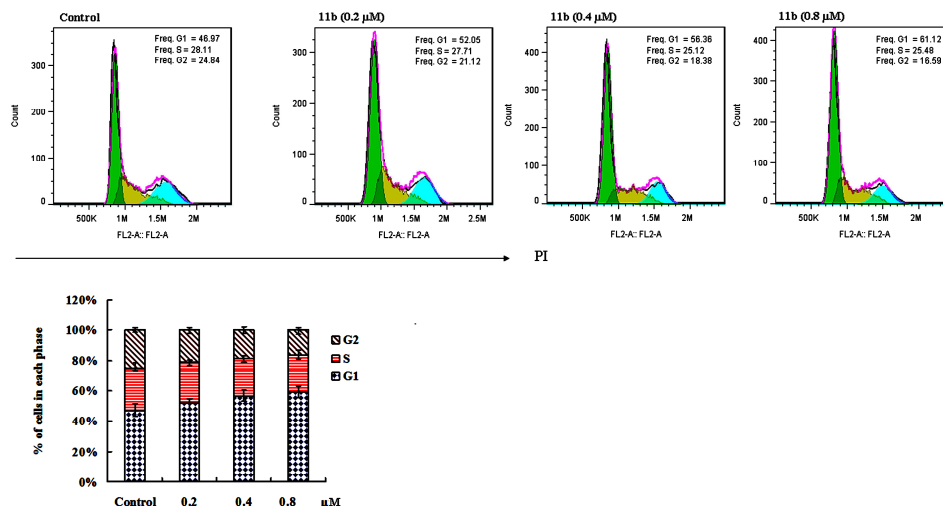


**Fig. 7.** Cell cycle analysis of **11b** in A549 cells. Cells were treated with **11b** at 0.2, 0.4 and 0.8 μM for 24 h, harvested, stained with PI, and then analyzed by flow cytometry.

### 3. Conclusion

Based on the strategy of creating multifunctional drugs, 11 new NO-releasing celastrol hybrids were designed and synthesized. Their anti-proliferative activities were evaluated against A549, HOS, MCF-7 and HepG2 cells. The intracellular NO productions of all the hybrids were tested *in vitro*. The NO release amounts detection indicated that there was a positive correlation between their anti-proliferative activities and the NO release. Moreover, introductions of different types of NO donors to the structure of CEL brought different influences to the activity. In this study, **11b** showed the most potent activity in A549 cells. Further mechanism studies showed that **11b** induced apoptosis through inhibiting the activity of Hsp90, releasing high level of NO. These results showed that inhibition of Hsp90 and release of NO was synergistic in cancer cells. In conclusion, the current finding may provide a new insight for the design of celastrol derivatives to enhance the efficacy of candidates.

### 4. Experimental

#### 4.1. Chemistry

##### 4.1.1. General

All reagents were purchased from chemical and biological company.  $^1\text{H}$  NMR and  $^{13}\text{C}$  NMR spectra were recorded on a Bruker AVANCE instrument at  $25^\circ\text{C}$ . The molecular weights were detected on HP 1100LC/MSD spectrometer. Intermediates **7a-e**, **8a-8e**, **10a-b** and **12a-12d** were synthesized according to the previous methods.

#### 4.1.2. General procedure for synthesis of **9a-9e**

**8a-e** (0.11 mM, 1.1 eq) and **1** (0.10 mM, 1 eq) were dissolved in DMF (5.0 mL). Then  $\text{NaHCO}_3$  (0.50 mM) was added. The solution was stirred for 12 h at  $25^\circ\text{C}$ . The reaction mixture was then diluted with  $\text{CH}_2\text{Cl}_2$ , washed with water, and dried over anhydrous  $\text{Na}_2\text{SO}_4$ , and concentrated. The residue was purified by flash column chromatography using PE/EA (6:1, v/v) as an eluent to afford **9a-9e**.

##### 4.1.2.1. **9a**

Red solid, yielded 49%. mp  $155.5\text{-}157.2^\circ\text{C}$ .  $^1\text{H}$  NMR (300 MHz,  $\text{CDCl}_3$ )  $\delta$ : 8.04 (2H, d,  $J = 7.3$  Hz), 7.75 (1H, t,  $J = 7.3$  Hz), 7.59 (2H, t,  $J = 7.4$  Hz), 6.89 (1H, d,  $J = 6.7$  Hz), 6.53 (1H, s), 6.34 (1H, d,  $J = 7.0$  Hz), 4.60 (2H, m), 3.95-4.14 (2H, m), 2.18 (3H, s), 1.45 (3H, s), 1.27 (3H, s), 1.23 (3H, s), 1.12 (3H, s), 0.60 (3H, s).  $^{13}\text{C}$  NMR (75 MHz,  $\text{CDCl}_3$ )  $\delta$ : 178.3, 178.2, 170.0, 164.8, 158.7, 146.0, 138.0, 135.7 (C $\times$ 2), 134.2, 129.7 (C $\times$ 2), 128.4 (C $\times$ 2), 127.3, 119.6, 118.2, 117.1, 68.7, 61.4, 45.0, 44.2, 42.9, 40.6, 39.4, 38.3, 36.3, 36.4, 33.6, 32.8, 31.6, 31.0, 30.6, 29.7 (C $\times$ 2), 28.6, 21.6, 18.7, 10.3. HRMS (ESI) calculated for  $\text{C}_{39}\text{H}_{47}\text{N}_2\text{O}_9\text{S}$   $[\text{M} + \text{H}]^+$  719.2999, found 719.3002.

##### 4.1.2.2. **9b**

Red solid, yielded 56%. mp  $186.0\text{-}187.4^\circ\text{C}$ .  $^1\text{H}$  NMR (300 MHz,  $\text{CDCl}_3$ )  $\delta$ : 7.98 (2H, d,  $J = 7.7$  Hz), 7.70 (1H, d,  $J = 7.0$  Hz), 7.60 (2H, t,  $J = 7.4$  Hz), 7.03 (1H, d,  $J = 6.9$  Hz), 6.51 (1H, s), 6.35 (1H, d,  $J = 6.9$  Hz), 4.49 (2H, d,  $J = 7.2$  Hz), 4.04-4.13 (2H, m), 2.21 (3H, s), 1.45 (3H, s), 1.29 (3H, s), 1.19 (3H, s), 1.11 (3H, s), 0.54 (3H, s).  $^{13}\text{C}$  NMR (75 MHz,  $\text{CDCl}_3$ )  $\delta$ : 178.3, 178.2, 169.7, 164.6, 158.8, 146.0, 137.9, 135.6, 134.2, 129.7 (C $\times$ 2), 128.4 (C $\times$ 2), 127.4 119.4, 118.2, 117.2, 67.9, 60.2, 45.0, 44.2, 42.9, 40.5, 39.5, 38.2, 36.3, 34.9, 33.6, 32.9, 31.6, 31.5, 30.9, 29.7 (C $\times$ 2), 28.6, 27.7, 21.6, 18.5, 10.3. HRMS (ESI) calculated for  $\text{C}_{40}\text{H}_{49}\text{N}_2\text{O}_9\text{S}$   $[\text{M} + \text{H}]^+$  733.3159, found 733.3157.

#### 4.1.2.3. **9c**

Red solid, yielded 58%. mp 156.1-157.8 °C.  $^1\text{H}$  NMR (300 MHz,  $\text{CDCl}_3$ )  $\delta$ : 8.05 (2H, d,  $J = 7.4$  Hz), 7.76 (1H, d,  $J = 7.4$  Hz), 7.62 (2H, t,  $J = 7.0$  Hz), 7.02 (1H, d,  $J = 7.0$  Hz), 6.54 (1H, s), 6.36 (1H, d,  $J = 7.1$  Hz), 4.46 (2H, t,  $J = 6.2$  Hz), 3.92-4.14 (2H, m), 2.21 (3H, s), 1.46 (3H, s), 1.28 (3H, s), 1.21 (3H, s), 1.12 (3H, s), 0.59 (3H, s).  $^{13}\text{C}$  NMR (75 MHz,  $\text{CDCl}_3$ )  $\delta$ : 178.3 (C $\times$ 2), 169.97, 164.7, 158.9, 146.0, 135.6, 134.2, 129.7 (C $\times$ 3), 127.4 (C $\times$ 3), 119.5, 118.2, 117.1, 70.9, 63.6, 45.1, 44.2, 42.9, 40.5, 39.4, 38.2, 36.3, 34.8, 33.5, 32.9, 31.6, 30.9, 30.6, 29.8, 29.7, 25.4, 24.9, 21.6, 18.6, 14.1, 10.3. HRMS (ESI) calculated for  $\text{C}_{41}\text{H}_{51}\text{N}_2\text{O}_9\text{S}$  [ $\text{M} + \text{H}$ ] $^+$  747.3315, found 747.3316.

#### 4.1.2.4. **9d**

Red solid, yielded 55%. mp 164.3-165.3 °C.  $^1\text{H}$  NMR (300 MHz,  $\text{CDCl}_3$ )  $\delta$ : 8.05 (2H, d,  $J = 7.8$  Hz), 7.75 (1H, d,  $J = 7.4$  Hz), 7.63 (2H, t,  $J = 7.9$  Hz), 7.02 (1H, d,  $J = 7.1$  Hz), 6.54 (1H, s), 6.35 (1H, d,  $J = 7.1$  Hz), 4.75 (1H, t,  $J = 3.3$  Hz), 3.36-4.48 (2H, m), 2.22 (3H, s), 1.47 (3H, s), 1.46 (3H, d,  $J = 6.3$  Hz), 1.29 (3H, s), 1.22 (3H, s), 1.13 (3H, s), 0.63 (3H, s).  $^{13}\text{C}$  NMR (75 MHz,  $\text{CDCl}_3$ )  $\delta$ : 179.6, 178.7, 169.7, 164.6, 158.8, 146.0, 137.6, 135.6, 134.2, 129.7 (C $\times$ 2), 128.5 (C $\times$ 2), 127.4, 124.4, 119.4, 118.2, 72.4, 67.6, 45.0, 42.9, 40.6, 38.2, 36.3, 34.9, 33.2, 31.5, 30.7, 30.6, 29.6 (C $\times$ 2), 28.7, 21.7, 21.6, 19.0, 18.8, 16.0, 10.2. HRMS (ESI) calculated for  $\text{C}_{40}\text{H}_{49}\text{N}_2\text{O}_9\text{S}$  [ $\text{M} + \text{H}$ ] $^+$  733.3159, found 733.3166.

#### 4.1.2.5. **9e**

Red solid, yielded 50%. mp 173.8-175.0 °C.  $^1\text{H}$  NMR (300 MHz,  $\text{CDCl}_3$ )  $\delta$ : 8.00 (2H, d,  $J = 7.1$  Hz), 7.74 (1H, d,  $J = 7.3$  Hz), 7.59 (2H, t,  $J = 8.0$  Hz), 7.03 (1H, d,  $J = 7.1$  Hz), 6.50 (1H, s), 6.35 (1H, d,  $J = 7.2$  Hz), 4.35 (2H, t,  $J = 5.3$  Hz), 3.82-4.12 (2H, m), 2.22 (3H, s), 1.44 (3H, s), 1.29 (3H, d,  $J = 7.3$  Hz), 1.28 (3H, s), 1.19 (3H, s), 1.12 (3H, s), 0.54 (3H, s).  $^{13}\text{C}$  NMR (75 MHz,  $\text{CDCl}_3$ )  $\delta$ : 178.2, 178.1, 169.9, 164.7, 146.0, 138.0, 135.6, 134.4, 129.7 (C $\times$ 3), 128.5 (C $\times$ 3), 127.4, 119.5, 118.2, 72.4, 65.3, 45.0, 44.3, 42.9, 40.6, 39.5, 38.2, 36.3, 34.9, 33.6, 32.8, 32.4, 31.6, 30.57, 29.7, 28.6, 21.6, 18.5, 13.8, 13.7, 10.2. HRMS (ESI) calculated for  $\text{C}_{41}\text{H}_{51}\text{N}_2\text{O}_9\text{S}$  [ $\text{M} + \text{H}$ ] $^+$  747.3315, found 747.3315.

#### 4.1.3. General procedure for synthesis of **11a-11b**

**10a-b** (0.11 mmol, 1.1 eq) were respectively added to a solution of **1** (0.10 mmol, 1 eq), PyBop (0.20 mmol) and hung's base (0.25 mmol) in CH<sub>2</sub>Cl<sub>2</sub> (5.0 mL). The suspension was stirred at room temperature (10 h). The filtrate was evaporated under reduced pressure. The resulting crude product was purified by column chromatography (PE/EA = 3:1 v/v) to generate **11a-11b**.

#### 4.1.3.1. **11a**

Red solid, yielded 46%. mp 151.1-152.6 °C. <sup>1</sup>H NMR (300 MHz, CDCl<sub>3</sub>) δ: 8.03 (2H, d, *J* = 7.5 Hz), 7.78 (1H, d, *J* = 7.3 Hz), 7.62 (2H, t, *J* = 7.9 Hz), 7.02 (1H, d, *J* = 6.5 Hz), 6.50 (1H, s), 6.33 (1H, d, *J* = 7.2 Hz), 4.44 (2H, m), 3.52-3.78 (2H, m), 2.23 (3H, s), 1.45 (3H, s), 1.28 (3H, s), 1.21 (3H, s), 1.15 (3H, s), 0.64 (3H, s). <sup>13</sup>C NMR (75 MHz, CDCl<sub>3</sub>) δ: 178.8, 178.3, 170.6, 165.0, 146.0, 139.2, 135.8, 134.5, 129.8 (C×3), 128.3 (C×3), 121.9, 119.4, 118.2, 70.0, 45.0, 44.3, 43.0, 40.6, 39.4, 38.6, 38.2, 36.3, 34.8, 33.8, 33.6, 31.6, 31.0, 30.9, 30.0, 29.4, 28.7, 21.6, 18.4, 10.3. HRMS (ESI) calculated for C<sub>39</sub>H<sub>48</sub>N<sub>3</sub>O<sub>8</sub>S [M + H]<sup>+</sup> 718.3162, found 718.3157.

#### 4.1.3.2. **11b**

Red solid, yielded 42%. mp 146.2-147.8 °C. <sup>1</sup>H NMR (300 MHz, CDCl<sub>3</sub>) δ: 8.03 (2H, d, *J* = 7.9 Hz), 7.77 (1H, d, *J* = 7.5 Hz), 7.63 (2H, t, *J* = 7.9 Hz), 7.02 (1H, d, *J* = 7.1 Hz), 6.53 (1H, s), 6.53 (1H, d, *J* = 7.5 Hz), 4.45 (2H, t, *J* = 5.9 Hz), 3.36-3.39 (2H, m), 2.06 (3H, s), 1.35 (3H, s), 1.27 (3H, s), 1.19 (3H, s), 1.14 (3H, s), 0.66 (3H, s). <sup>13</sup>C NMR (75 MHz, CDCl<sub>3</sub>) δ: 178.3, 178.2, 169.8, 164.7, 146.0, 139.0, 134.1, 131.7, 129.3 (C×3), 128.8 (C×3), 127.0, 119.5, 118.2, 117.1, 70.3, 45.1, 44.3, 43.0, 40.5, 39.4, 38.2, 36.3 (C×3), 34.8, 33.4, 32.8, 31.6, 30.8, 30.5, 29.7, 28.6, 21.7, 18.6, 14.1, 10.3. HRMS (ESI) calculated for C<sub>40</sub>H<sub>50</sub>N<sub>3</sub>O<sub>8</sub>S [M + H]<sup>+</sup> 732.3319, found 732.3320.

#### 4.1.4. General procedure for synthesis of **13a-13d**

To a solution of **12a-d** (0.10 mmol, 1eq) in CH<sub>3</sub>CN (5.0 mL) was added AgNO<sub>3</sub> (0.15 mmol, 1.5 eq). After 10 h stirring at 80 °C in the darkness, the filtrate was evaporated under reduced pressure. The crude product was purified by column chromatography (PE/EA = 10:1 v/v) to give **13a-13d**.

#### 4.1.4.1. **13a**

Red solid, yielded 50%. mp 165.3-166.6 °C. <sup>1</sup>H NMR (300 MHz, CDCl<sub>3</sub>) δ:

7.03(1H, d,  $J = 7.2$  Hz), 6.55 (1H, s), 6.36 (1H, d,  $J = 7.1$  Hz), 4.54 (2H, m), 3.95-4.14 (2H, m), 2.23 (3H, s), 1.44 (3H, s), 1.30 (3H, s), 1.27 (3H, s), 1.12 (3H, s), 0.56 (3H, s).  $^{13}\text{C}$  NMR (75 MHz,  $\text{CDCl}_3$ )  $\delta$ : 178.3, 178.2, 170.2, 164.8, 146.0, 134.2, 128.4, 119.4, 118.2, 117.3, 71.6, 64.8, 50.2, 44.3, 40.4, 39.4, 38.2, 36.3, 34.7, 33.6, 32.7, 31.6, 30.7, 30.5, 29.8, 29.6, 28.6, 28.2, 26.2, 25.7, 21.6, 18.4, 10.2. HRMS (ESI) calculated for  $\text{C}_{32}\text{H}_{44}\text{NO}_7$   $[\text{M} + \text{H}]^+$  544.3118, found 544.3120.

#### 4.1.4.2 **13b**

Red solid, yielded 59%. mp 166.1-167.7 °C.  $^1\text{H}$  NMR (300 MHz,  $\text{CDCl}_3$ )  $\delta$ : 7.04 (1H, d,  $J = 6.6$  Hz), 6.56 (1H, s), 6.36 (1H, d,  $J = 6.8$  Hz), 4.50 (2H, t,  $J = 6.41$  Hz), 3.88-4.04 (2H, m), 2.23 (3H, s), 1.47 (3H, s), 1.28 (3H, s), 1.27 (3H, s), 1.12 (3H, s), 0.56 (3H, s).  $^{13}\text{C}$  NMR (75 MHz,  $\text{CDCl}_3$ )  $\delta$ : 178.2 (C $\times$ 2), 173.3, 165.4, 147.1, 134.1, 127.6, 119.9 (C $\times$ 2), 118.2, 72.5, 63.5, 45.0, 44.2, 42.9, 40.4, 38.3, 36.3, 34.7, 33.5, 32.8, 31.6, 30.8, 30.5, 30.2, 29.8, 29.7 (C $\times$ 2), 28.6, 24.8, 23.8, 21.6, 18.5, 10.3. HRMS (ESI) calculated for  $\text{C}_{33}\text{H}_{46}\text{NO}_7$   $[\text{M} + \text{H}]^+$  568.3274, found 568.3273.

#### 4.1.4.3. **13c**

Red solid, yielded 46%. mp 170.4-171.8 °C.  $^1\text{H}$  NMR (300 MHz,  $\text{CDCl}_3$ )  $\delta$ : 7.04 (1H, d,  $J = 6.96$  Hz), 6.55 (1H, s), 6.36 (1H, d,  $J = 6.84$  Hz), 4.47 (2H, t,  $J = 6.45$  Hz), 3.85-4.04 (2H, m), 2.23 (3H, s), 1.44 (3H, s), 1.30 (3H, s), 1.27 (3H, s), 1.12 (3H, s), 0.56 (3H, s).  $^{13}\text{C}$  NMR (75 MHz,  $\text{CDCl}_3$ )  $\delta$ : 178.6, 178.3, 167.1, 165.0, 146.3, 134.4, 128.4, 119.9, 118.5, 118.0, 71.4, 61.3, 45.4, 44.6, 43.3, 40.8, 39.8, 38.5, 36.7, 35.2, 33.7, 33.1, 31.9, 31.8, 31.1, 30.8, 30.5, 30.1, 30.0, 28.9, 28.2, 22.0, 18.9, 10.6. HRMS (ESI) calculated for  $\text{C}_{34}\text{H}_{48}\text{NO}_7$   $[\text{M} + \text{H}]^+$  582.3431, found 582.3436.

#### 4.1.4.4. **13d**

Red solid, yielded 41%. mp 169.3-171.1 °C.  $^1\text{H}$  NMR (300 MHz,  $\text{CDCl}_3$ )  $\delta$ : 6.99 (1H, d,  $J = 7.11$  Hz), 6.32 (1H, s), 5.09 (1H, d,  $J = 8.01$  Hz), 4.34 (2H, t,  $J = 6.51$  Hz), 3.71-4.03 (2H, m), 1.95 (3H, s), 1.35 (3H, s), 1.20 (3H, s), 1.12 (3H, s), 0.99 (3H, s), 0.61 (3H, s).  $^{13}\text{C}$  NMR (75 MHz,  $\text{CDCl}_3$ )  $\delta$ : 178.9, 178.7, 172.5, 150.9, 142.8, 130.0, 126.2, 120.0, 119.9, 73.1, 64.2, 46.4, 45.8, 41.4, 40.4, 39.2, 37.4, 36.6, 32.9, 31.6, 31.4, 31.2, 30.6, 29.7, 29.6, 28.2, 26.8, 26.7, 25.7, 25.1, 23.3, 19.4, 18.9, 10.9. HRMS (ESI) calculated for  $\text{C}_{35}\text{H}_{50}\text{NO}_7$   $[\text{M} + \text{H}]^+$  596.3587, found 596.3588.

## 4.2. Biological experiments

### 4.2.1. Cytotoxic assay *in vitro*

All hybrids were evaluated for their inhibitory activities against A549, MCF-7, HOS and HepG2 by MTT method. Briefly, 100  $\mu\text{L}$  of each cell ( $5.0 \times 10^4$  cells/ml) were seeded into 96-well plates and incubated for 24 h. Different concentrations of the drug were added into the 96-well plates. Then these plates were incubated for 48 h. MTT solution (5 mg/ml) was added, and cultured (4 h). Supernatant was abandoned before adding 100  $\mu\text{L}$  DMSO to each well. The OD at 570 nm was measured using a microplate reader (POLARstar Omega, Offenburg, Germany). Every assay was performed in triplicate. Data are presented as the mean  $\pm$  SD ( $n = 3$ ).

### 4.2.2. NO release amounts detection

NO release amounts *in vitro* were calculated by Nitrate/Nitrite Assay Kit (KeyGEN, China). Firstly, A549 cells ( $3 \times 100 \mu\text{L}$ ,  $5.0 \times 10^4$  cells/ml) were incubated in 96 well-plates for 24 h at 37 °C and then treated with the indicated hybrids (4  $\mu\text{M}$ ) for different time. Secondly, the amounts of NO *in vitro* were measured according to the manufacturer's instructions. The OD at 550 nm was measured using a microplate reader (POLARstar Omega, Offenburg, Germany). Data were mean of three independent experiments.

### 4.2.3. Western blotting analysis

A549 cells were seeded ( $5 \times 10^5$  cells) in 6 cm dishes and incubated with 24 h. **11b** was added to the dishes with indicated concentration and then these dishes were incubated for another 24 h. The cells were washed and lysed using lysis buffer. The lysates were centrifuged at 10,000  $g$  for 20 min at 4 °C. Then the proteins were diluted to 3 mg/ml (BCA method). Each sample (10  $\mu\text{L}$ ) was analyzed by SDS-PAGE (10 % gel). Then the proteins were detected by the conventional method. The monoclonal antibodies were purchased (Abcam, Cambridge, UK).

### 4.2.4. Cell cycle analysis

A549 cells ( $4 \times 10^5$  cells) were incubated in 6 cm dishes for 24 h. Then **11b** and **1** were added to the dishes with different concentrations. After incubation of 24 h, the cells were harvested and washed twice with cold PBS. Then the cell was fixed in

ethanol (75 %) at - 20 °C for at least 12 h. The cells were washed with buffer A to remove the ethanol. The cells were followed suspended in buffer A (250 µL) containing 250 mg/ml RNase A and cultured at 37 °C for 30 min. Finally, 2.5 µL propidium iodide (PI) (KeyGEN, China) was added and incubated at room temperature in dark for 15 min. The cells were analyzed by flow cytometry (BD Accuri C6 flow cytometer, Franklin Lakes, NJ).

#### 4.2.5. Cell apoptosis analysis

A549 cells ( $4 \times 10^5$  cells) were incubated in 6 cm dish for 24 h. Then **11b** and **1** were added to the cells with indicated concentrations. After another incubation of 48 h, the cells were harvested softly and washed twice with cold PBS (2000 g for 5 min). Then the cells were added to 250 µL binding buffer containing 2.5 µL PI and 2.5 µL Annexin V (KeyGEN, China). The mixture was incubated at room temperature for 15 min in the darkness and analyzed by flow cytometry.

#### 4.2.6. Hoechst-33342-staining

A549 cells ( $4 \times 10^5$  cells) were incubated in 6 cm dish for 24 h. Then A549 cells were treated with the **11b** at indicated concentrations for 48 h. Cells were washed twice by PBS. Then cells were incubated with Hoechst-33342 (10 µg/ml) for 5 min at room temperature in the darkness. After incubation, stained cells were observed under a fluorescent microscope (CORPORATION, Japan).

### Acknowledgements

This work was financially supported by the Academic Innovation Project of Jiangsu Department of Education (No. 1131740036).

### Appendix A. Supplementary data

Supplementary data related to this article can be found at.

### References

- [1] A. Salminen, M. Lehtonen, T. Paimela, K. Kaarniranta. *Biochem. Biophys. Res. Commun.* 394 (2010) 439-442.
- [2] S.A.C. Figueiredo, J.A.R. Salvador, R. Cortés, M. Cascante. *Eur. J. Med. Chem.* 139 (2017) 836-848.

- [3] W. Tang, J. Wang, X. Tong, J. Shi, X. Liu, J. Li. *Eur. J. Med. Chem.* 95 (2015) 166-173.
- [4] T. Zhang, Y. Li, Y. Yu, P. Zou, Y. Jiang, D. Sun. *J. Biol. Chem.* 51 (2009) 35381-35389.
- [5] T. Zhang, A. Hamza, X. Cao, B. Wang, S. Yu, C. Zhan, D. Sun. *Mol. Cancer Ther.* 7 (2008) 162-170.
- [6] S.M. Roe, M.M. Ali, P. Meyer, C.K. Vaughan, B. Panaretou, P.W. Piper, C. Prodromou, L.H. Pearl. *Cell* 116 (2004) 87-98.
- [7] L. Whitesell, S.L. Lindquist. *Nat. Rev. Cancer* 5 (2005) 761-772.
- [8] L. H. Pearl, *Curr. Opin. Genet. Dev.* 15 (2005) 55-61.
- [9] B. Bonavida, S. Khineche, S. Huerta-Yepez, H. Garban. *Updates* 9 (2006) 157-173.
- [10] B. Bonavida, S. Baritaki, S. Huerta-Yepez, M.I. Vega, D. Chatterjee, K. Yeung. *Nitric Oxide* 19 (2008) 152-157.
- [11] Z. Huang, J. Fu, Y. Zhang. *J. Med. Chem.* 60 (2017) 7617-7635.
- [12] B. Bonavida, S. Khineche, S. Huerta-Yepez, H. Garban. *Drug Resist. Updates* 9 (2006) 157-173.
- [13] R. Alexandrova, M. Mileva, E. Zvetkova. *Exp. Pathol. Parasitol* 4 (2001) 13-18.
- [14] X. Gu, Z. Huang, Z. Ren, X. Tang, R. Xue, X. Luo, S. Peng, Hui Peng, B. Lu, J. Tian, Y. Zhang. *J. Med. Chem.* (60) 2017, 928-940.
- [15] G. Aguirre, M. Boiani, H. Cerecetto, M. Fernández, M. González, E. León, C. Pintos, S. Raymondo, C. Arredondo, J.P. Pacheco, M.A. Basombrío. *Pharmazie* 61 (2006) 54-59.
- [16] M.A.E. Mourad, M. Abdel-Aziz, G.E.D.A.A. Abuo-Rahma, H.H. Farag. *Eur. J. Med. Chem.* 54 (2012) 907-913.
- [17] Y. Ai, F.H. Kang, Z.J. Huang, X.W. Xue, Y.S. Lai, S.X. Peng, J.D. Tian, Y.H. Zhang. *J. Med. Chem.* 58 (2015) 2452-2464.
- [18] N. Zhao, K.T. Tian, K.G. Cheng, T. Han, X. Hu, D.H. Li, Z.L. Li, H.M. Hua. *Bioorg. Med. Chem.* 24 (2016) 2971-2978.
- [19] J. Chen, T. Wang, S. Xu, P. Zhang, A. Lin, L. Wu, H. Yao, W. Xie, Z. Zhu, J. Xu.

- Eur. J. Med. Chem. 135 (2017) 414-423.
- [20] N. Kerru, P. Singh, N. Koorbanally, R. Raj, V. Kumar. Eur. J. Med. Chem. 142 (2017) 179-212.
- [21] P. Klahn, M. Brönstrup. Nat. Prod. Rep. 34 (2017) 832-885.
- [22] K. Singh, V. Verma, K. Yadav, V. Sreekanth, D. Kumar, A. Bajaj, V. Kumar. Eur. J. Med. Chem. 87 (2014) 150-158.
- [23] Y. Garazd, M. Garazd, R. Lesyk Saudi. Pharm. J. 25 (2017) 214-223.
- [24] Z. Huang, J. Wu, Y. Zou, H. Yuan, Y. Zhang, Y. Fei, A. Bhardwaj, J. Kaur, E.E. Knaus, Y. Zhang. J. Med. Chem. 61 (2018) 1833-1844.
- [25] L. Chen, Y. Zhang, X. Kong, E. Lan, Z. Huang, S. Peng, D.L. Kaufman, J. Tian. J. Med. Chem. 51 (2008) 4834-4838.
- [26] Z. Huang, Y. Zhang, L. Zhao, Y. Jing, Y. Lai, L. Zhang, Q. Guo, S. Yuan, J. Zhang, L. Chen, S. Peng, J. Tian. Org. Biomol. Chem. 8 (2010), 632-639.
- [27] Y. Ai, F.H. Kang, Z.J. Huang, X.W. Xue, Y.S. Lai, S.X. Peng, J.D. Tian, Y. H. Zhang. J. Med. Chem. 58 (2015) 2452-2464.
- [28] Y. Lai, L. Shen, Z. Zhang, W. Liu, Y. Zhang, H. Ji, J. Tian. Bioorg. Med. Chem. Lett. 20 (2010) 6416-6420.
- [29] N. Bao, J. Ou, M. Xu, F. Guan, W. Shi, J. Sun, L. Chen. Eur. J. Med. Chem. 137 (2017) 88-95.
- [30] K.M. Miranda, M.G. Espey, D.A. Wink. Nitric Oxide 5 (2001) 62-71.
- [31] F. Jiang, H.J. Wang, Q.C. Bao, L. Wang, Y.H. Jin, Q. Zhang, D. Jiang, Q.D. You, X.L. Xu. Bioorg. Med. Chem. 24 (2016) 5431-5439.
- [32] P. Tongkate, W. Pluempanupat, W. Chavasiri. Tetrahedron Letters 49 (2008) 1146-1148.
- [33] L. Chen, Y. Zhang, X. Kong, S. Peng, J. Tian. Bioorg. Med. Chem. Lett. 17 (2007) 2979-2982.
- [34] F. Amano, T. Noda. FEBS Lett. 368 (1995) 425-428.
- [35] A. Chadli, S.J. Felts, Q. Wang, W.P. Sullivan, M. Victoria Botuyan, A. Fauq, M. Ramirez-Alvarado, G. Mer. J. Biol. Chem. 6 (2010) 4224-4231.
- [36] S. Sreeramulu, H.R.A. Jonker, T. Langer, C. Richter, C. Roy D. Lancaste, H.

Schwalbe. J. Biol. Chem. 6 (2006) 3885-3896.

[37] S. Sreeramulu, S.L. Gande, M. Göbel, H. Schwalbe. Angewandte Chemie 48 (2009) 5853-5855.

ACCEPTED MANUSCRIPT

**Figure captions**

**Fig. 1.** Effects of NO produced by the target compounds on A549 cell proliferation. (A) NO release amounts of partial hybrids producing *vs.* time. A549 cells were treated with 4  $\mu$ M of the selected compounds for different hours (mean  $\pm$  SD, n = 3). (B) The levels of NO produced by all of the compounds in A549 cells. A549 cells were treated with 4  $\mu$ M of all the hybrids for 24 hours (mean  $\pm$  SD, n = 3).

**Fig. 2.** Effect of PTIO on the anti-proliferative activity of **11b**. A549 cells were pretreated with the indicated concentrations of PTIO for 2 h and then treated with 4  $\mu$ M of **11b** for another 24 h. Data were expressed as the mean  $\pm$  SD (n=3). \*  $P < 0.05$ , \*\*  $P < 0.01$  *vs.* the group without PTIO.

**Fig. 3.** Effects of **11b** on Hsp90 clients in A549 cells. A549 cells were treated with varying concentrations of **11b** for 24 h. (A) The expressions of Cdk-4 and Hsp90 were determined by Western Blotting using specific antibodies.  $\beta$ -actin was used as internal control; (B) The expressions of *p*-Akt and Akt were determined by Western Blotting using specific antibodies.

**Fig. 4.** Anti-proliferative activity of **11b** in comparison with that of **1**, **10b** and their mixture in A549 cells.

**Fig. 5.** Fluorescence microscopy images of A549 cells stained by Hoechst 33342. A549 cells were treated with the **11b** at indicated concentrations for 48 h.

**Fig. 6.** Effect of **11b** on apoptosis of A549 cells. (A) A549 cells were treated with **11b** at the indicated concentrations for 48 h. Apoptotic effects were measured by flow cytometry using Annexin V-FITC/PI staining protocol; (B) Representative histograms for the numbers of cells (% of total) in the early and late stages of apoptosis for the treatment groups.

**Fig. 7.** Cell cycle analysis of **11b** in A549 cells. Cells were treated with **11b** at 0.2, 0.4 and 0.8  $\mu$ M for 24 h, harvested, stained with PI, and then analyzed by flow cytometry.

- A series of celastrol/NO donor hybrids were designed, synthesized and evaluated.
- **11b** exhibited superior potency compared to the other compounds.
- **11b** induced degradation of the Hsp90 clients (Akt and Cdk4), apoptosis and the cell cycle arrested at the G<sub>0</sub>/G<sub>1</sub> phase in A549 cells.